Cite as: Zhang L, Nan Z, Liang X, Xu Y, Hernandez F, Li L. Application of the MacCormack Scheme to Overland Flow Routing for High-spatial Resolution Distributed Hydrological Model. Journal of Hydrology. 2018, 558: 421-431.

Application of the MacCormack scheme to overland flow routing for high-spatial resolution distributed hydrological model

Ling Zhang[1], Zhuotong Nan[2*], Xu Liang[3*], Yi Xu[4], Felipe Hernandez[3], Lianxia Li[5]

[1] Key Laboratory of Remote Sensing of Gansu Province, Northwest Institute of Eco-Environment and Resources, Chinese Academy of Sciences, 730000, Lanzhou, China

[2] Ministry of Education Key Laboratory of Virtual Geographic Environment, Nanjing Normal University, Nanjing 210023, China

[3] Department of Civil and Environmental Engineering, University of Pittsburgh, Pittsburgh, PA 15261, USA

[4] Jiangsu Center for Collaborative Innovation in Geographical Information Resource Development and Application, Nanjing 210023, China

[5] College of Hydraulic & Hydroelectric Engineering, Sichuan University, Chengdu 610065, China

* Corresponding author. Email: nanzt@njnu.edu.cn, xuliang@pitt.edu

ABSTRACT: Although process-based distributed hydrological models (PDHMs) are evolving rapidly over the last few decades, their extensive applications are still challenged by the computational expenses. This study attempted, for the first time, to apply the numerically efficient MacCormack algorithm to overland flow routing in a

representative high-spatial resolution PDHM, i.e., the distributed hydrology-soil-vegetation model (DHSVM), in order to improve its computational efficiency. The analytical verification indicates that both the semi and full versions of the MacCormack schemes exhibit robust numerical stability and are more computationally efficient than the conventional explicit linear scheme. The full-version outperforms the semi-version in terms of simulation accuracy when a same time step is adopted. The semi-MacCormack scheme was implemented into DHSVM (version 3.1.2) to solve the kinematic wave equations for overland flow routing. The performance and practicality of the enhanced DHSVM-MacCormack model was assessed by performing two groups of modeling experiments in the Mercer Creek watershed, a small urban catchment near Bellevue, Washington. The experiments show that DHSVM-MacCormack can considerably improve the computational efficiency without compromising the simulation accuracy of the original DHSVM model. More specifically, with the same computational environment and model settings, the computational time required by DHSVM-MacCormack can be reduced to several dozen minutes for a simulation period of three months (in contrast with one day and a half by the original DHSVM model) without noticeable sacrifice of the accuracy. The MacCormack scheme proves to be applicable to overland flow routing in DHSVM, which implies that it can be coupled into other PHDMs for watershed routing to either significantly improve their computational efficiency or to make the kinematic wave routing for high resolution modeling computational

feasible.

Keywords: MacCormack scheme; Overland flow routing; DHSVM; Kinematic wave; Computational efficiency

1 Introduction

Overland flow is one of the major components of the hydrological cycle and has the most intimate interactions with human beings because of their coexistence in space and time (Wong, 2011). It is normally unsteady and non-uniform and, therefore, can be described by the St. Venant equations. Owing to the highly nonlinear nature of these equations which involve a high degree of complexity in their computation, various approximations of the St. Venant equations have been proposed for solving overland flow problems. The kinematic wave (KW) model, which was first developed by Lighthill and Whitham (1955), is one of such approximations and proves to be adequate for most practical overland flow situations (Akan and Houghtalen, 2003). The major assumption of the KW model is that the acceleration and pressure terms in the momentum equation are insignificant and, consequently, the friction slope is equal to the terrain slope (Miller, 1984). The KW model is essentially a set of nonlinear hyperbolic partial differential equations for which analytical solutions cannot be obtained except for a few idealized conditions. The finite difference (FD) numerical methods, which are generally classified into explicit and implicit schemes, are therefore frequently used to solve the KW equations. Both the explicit and implicit

FD methods have comparative strengths and weaknesses. The explicit FD schemes are easy to formulate and program, but are subjected to a necessary and insufficient condition for stability known as the Courant-Friedrichs-Lewy stability (CFL) condition (Chow et al., 1988). The CFL condition imposes a restriction on the workable time steps, which limits the computational efficiency and the practical applications of the explicit FD method. The implicit FD schemes, on the other hand, are unconditionally stable, but suffer from (i) high computational complexity due to the matrix operations; (ii) large memory demand; and (iii) deficiency in their applications to nonlinear problems (Kazezyılmaz-Alhan et al., 2005; Huang and Lee, 2013).

Process-based distributed hydrological models (PDHMs) are evolving rapidly over the last few decades (Paniconi and Putti, 2015). This is partly spurred by the tremendous advances in computing power, programming techniques and data availability; and partly by the increasing demands for spatially distributed hydrological simulations, impact assessments and interdisciplinary studies (Beven, 2011; Fenicia et al., 2016). Nevertheless, the extensive applications of PDHMs are still challenged by their computational burden since PDHMs are mostly associated with solving nonlinear partial differential equations over large domains at fine spatiotemporal resolutions (Fatichi et al., 2016). In PDHMs such as the distributed hydrology-soil-vegetation model (DHSVM) (Wigmosta et al., 1994), the geomorphology-based hydrological model (GBHM) (Yang, 1998), and the water flow

and balance simulation model (WaSiM) (Schulla and Jasper, 2007), the routing of overland flow is usually described by the KW equations, owing to its simplicity and satisfactory accuracy compared to the St. Venant equations (Jain and Singh, 2005; Tsai and Yang, 2005; Yu and Duan, 2014). However, the computational efficiency of these models would be strictly constrained in case of using the conventional explicit FD schemes to solve the KW equations, because it usually requires very small time increments to comply with the CFL condition. For example, DHSVM routes the KW overland flow with the explicit linear scheme. We have tested it using the model's test site data, which corresponds to a small urban watershed (31 km^2) at a spatial resolution of 30 m, and found that it needs almost 186 hours to complete a 2.25 years simulation. The test was carried out on a Lenovo notebook PC with an Intel Core i7-2620M CPU and 8 GB RAM.

Considering the complexity of the real world, and the strong spatial heterogeneity of land surface characteristics, more attentions are increasingly paid to high-spatial resolution PDHMs for a refined representation of hydrological processes (Ochoa-Rodriguez et al., 2015). The computational efficiency of PDHMs is even worse when they are applied to a large study domain with a high spatial resolution, since smaller spatial steps require much smaller time steps to achieve a stable solution to the KW equations with an explicit FD scheme. Thus, it is of great significance and practical importance to propose more efficient numerical methods to solve the KW equations for overland flow routing to reduce the computational cost.

The MacCormack FD method, which was initially proposed to solve the time-dependent compressive Navier-Stokes equations, is a popular and widely-used numerical algorithm in computational hydraulics (MacCormack, 2003; Tseng, 2010). Recently, some researchers have successfully applied the MacCormack algorithm to KW overland flow problems. Kazezyılmaz-Alhan et al. (2005) investigated the reliability of the explicit MacCormack scheme and compared it to the available analytical solutions and to a 4-point implicit FD method. They concluded that the MacCormack algorithm is computationally more efficient than the 4-point implicit method, although they are comparable in accuracy. Tseng (2010) applied the unconditionally stable implicit MacCormack scheme to solve the KW problem and demonstrated that it is a simple, accurate, highly stable, and greatly efficient solver. Huang and Lee (2013) reformulated the implicit MacCormack scheme and then applied it to two mountainous watersheds for 2D runoff simulations. They reported that the proposed method was significantly superior to the conventional algorithm in terms of computational efficiency.

These previous studies consistently revealed the clear advantage of the MacCormack scheme over the other conventional numerical methods for solving the KW equations. None of them, however, have tested the applicability and advantage of the MacCormack scheme with a PDHM. This study, therefore, applies the MacCormack scheme to the KW overland flow routing in a representative high-spatial resolution PDHM (i.e., the DHSVM model). More specifically, the

behaviors of the semi and full versions of the MacCormack schemes were evaluated against analytical solutions for two synthetic overland flow cases with uniform rainfalls. Then the semi-MacCormack algorithm was implemented into DHSVM to improve the efficiency of routing its overland flow. The performance and practicability of the enhanced DHSVM model (DHSVM-MacCormack) were examined by carrying out two groups of modeling experiments in a small urban watershed in Washington.

2 Methods

The method section is organized as follows. Sections 2.1 and 2.2 briefly introduce the KW model and the MacCormack numerical scheme, respectively. Section 2.3 describes the approach of implementing the MacCormack scheme into DHSVM. Finally, in Section 2.4, the methods of evaluating the performances of the MacCormack schemes are presented.

2.1 Kinematic wave

The 1D KW model for overland flow routing is defined by the following continuity and momentum equations.

Continuity Equation:

$$\frac{\partial Q}{\partial x} + \frac{\partial A}{\partial t} = q_e \tag{1}$$

where Q is the discharge, A is the cross-sectional area of flow, x is the downslope

distance, t is the time, and q_e is the rainfall excess rate per unit flow length.

Momentum Equation:

$$S_0 = S_f \tag{2}$$

in which S_o is the bed slope and S_f is the friction slope. The momentum equation can be expressed equivalently to the following relationship between Q and A.

$$A = \alpha Q^{\beta} \tag{3}$$

By combining Eq.2 with the Manning equation, Eq.3 can be derived as follows:

$$A = (\frac{np^{2/3}}{C_n \sqrt{S_f}})Q^{3/5} \tag{4}$$

where n is the Manning roughness coefficient; P is the wetted perimeter, which can be considered equal to flow width for shallow water flow; and C_n equals to 1 for metric units and 1.49 for English units. Thus, $\alpha = (nP^{2/3}/(C_n\sqrt{S_o}))^{3/5}$ and $\beta = 3/5$.

Differentiation of Eq. 3 with respect to t and substitution of this into Eq.1 gives:

$$\frac{\partial Q}{\partial x} + \alpha\beta Q^{\beta-1}\frac{\partial Q}{\partial t} = q_e \tag{5}$$

Combining Eq.5 with $dQ = \frac{\partial Q}{\partial x}dx + \frac{\partial Q}{\partial t}dt$, it can be easily obtained that:

$$c_k = \frac{dQ}{dA} = \frac{dx}{dt} = \frac{1}{\alpha\beta Q^{\beta-1}} \tag{6}$$

where c_k is the KW celerity.

2.2 MacCormack numerical scheme

The MacCormack scheme is a variation of the two-step Lax–Wendroff technique and belongs to the family of splitting methods. It has a second-order accuracy in time and space. The MacCormack scheme consists of two steps: a predictor step followed by a

corrector step (MacCormack, 1982; MacCormack, 2003). The spatial derivatives are approximated by forward differences in the predictor step, whereas they are approximated by backward differences in the corrector step. The implicit MacCormack scheme in delta form for approximating the KW equations is presented in Eqs. 7 and 8.

$$\text{Preditor step}\begin{cases} \Delta A_i^n = -\dfrac{\Delta t}{\Delta x}(Q_{i+1}^n - Q_i^n) + q_e \Delta t \\ (1+\dfrac{\lambda \Delta t}{\Delta x})\delta A_i^{n+1/2} = \Delta A_i^n + \dfrac{\lambda \Delta t}{\Delta x}\ \delta A_{i+1}^{n+1/2} \\ A_i^{n+1/2} = A_i^n + \delta A_i^{n+1/2} \end{cases} \tag{7}$$

$$\text{Corrector step}\begin{cases} \Delta A_i^{n+1/2} = -\dfrac{\Delta t}{\Delta x}(Q_i^{n+1/2} - Q_{i-1}^{n+1/2}) + q_e \Delta t \\ (1+\dfrac{\lambda \Delta t}{\Delta x})\delta A_i^{n+1} = \Delta A_i^{n+1/2} + \dfrac{\lambda \Delta t}{\Delta x}\delta A_{i-1}^{n+1} \\ A_i^{n+1} = \dfrac{1}{2}(A_i^n + A_i^{n+1/2} + \delta A_i^{n+1}) \end{cases} \tag{8}$$

where i and n are the spatial and temporal indices, respectively; Δt and Δx are temporal and spatial steps, respectively; ΔA is the change in the cross-sectional area of flow; δA is the iteration variable; and q_e is the rainfall excess rate per unit flow length. Note that the predictor step is first evaluated based on a backward sweep from the lower boundary (i.e., the greatest space index) to the upper boundary (i.e., the lowest space index); and the corrector step is then implemented through a sweep in a forward direction (Furst and Furmanek, 2011).

The method is unconditionally stable provided that the parameter λ is chosen so that:

$$\lambda \geq \max(|c_k| - \frac{\Delta x}{\Delta t}, 0)\alpha_{\text{mac}} \quad \alpha_{\text{mac}} \geq 0.5 \tag{9}$$

in which a_{mac} is a coefficient which mainly depends on the wave celerity and watershed characteristics (Huang and Lee, 2013). If Δt already satisfies the stability condition of the explicit FD method, i.e., $|c_k| - \Delta x / \Delta t < 0$, the right-hand side of the above inequality vanishes and λ can thus be chosen to be zero. The implicit MacCormack scheme reduces to the explicit one in this case.

2.3 DHSVM-MacCormack

DHSVM is a fully distributed physically-based time-continuous model predominantly designed for mountainous regions with complex terrain. It can provide an integrated and dynamic representation of the spatial patterns of snow cover, soil moisture, evapotranspiration, and runoff at a spatial resolution represented by the digital elevation model (DEM) (Wigmosta et al., 1994). DHSVM (version 3.1.2) was selected as a representative PDHM in this study, mainly because of the free availability of the source code as well as the test site data. DHSVM divides a watershed into computational grid cells centered on DEM nodes, each of which is assigned with appropriate vegetation characteristic and soil property. Using the grid cell as basic unit, DHSVM (i) estimates evapotranspiration using a two-layer canopy model; (ii) simulates snow accumulation and melt using a mass and energy balance model; (iii) describes unsaturated moisture movement through multiple rooting zone soil layers using Darcy's Law; (iv) routes lateral saturated subsurface flow through a cell-by-cell approach using either the kinematic or diffusion approximation; (v) routes

overland flow using either a cell-by-cell approach or the KW approach; and (vi) simulates channel flow using a robust linear storage routing algorithm. More details about the model are available in Wigmosta et al. (1994), Storck et al. (1998) and Wigmosta and Perkins (2001). DHSVM has been widely utilized in various research fields such as hydrological process simulation (Du et al., 2007; Cuo et al., 2008), hydrological impact assessment (Thanapakpawin et al., 2007; Cuo et al., 2009; Dickerson-Lange and Mitchell, 2014; Alvarenga et al., 2016), and sediment erosion and transport modeling (Doten et al., 2006; Lanini et al., 2009).

In DHSVM, overland flow is primarily generated through a saturation excess mechanism, despite that a relatively crude infiltration excess parameterization has been included (Cuo et al., 2008). The directions of overland flow are determined based on DEM using the four-direction (D4) algorithm which assigns flow from each grid cell to its four adjacent neighbors. For example, as illustrated in Figure 1, the outflow from pixel 5 is subdivided into the downslope neighboring pixels in the eastern and southern directions, i.e., cell 6 ($Q51$) and cell 8 ($Q52$). The proportion of outflow in each direction is assumed to be equal to the ratio of flow width in that direction to the total flow width. Essentially, this is consistent with the Digital Elevation Model Networks (DEMON) model which describes two-dimensional and aspect-driven flow movements (Costa-Cabral and Burges, 1994). The D4 approach allows the inflows to a certain cell originate from multiple up-gradient adjacent cells. For instance, the inflows to cell 5 include the outflows from upstream cells 2 ($Q22$)

and 4 ($Q41$).

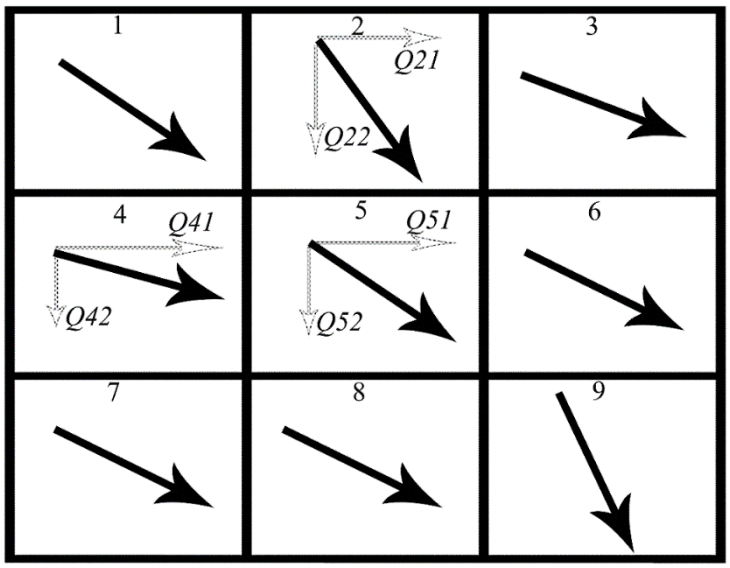

Figure 1. Illustration of DEM-based overland flow routing in DHSVM

The MacCormack scheme uses forward finite-differences for the spatial derivatives in the predictor step (Eq.7). When applying this scheme to the DEM-based overland flow routing system in DHSVM, it means that the variable $A_i^{n+1/2}$ at the current grid (i) needs to be estimated using the iteration variables (Q_{i+1}^n, $\delta A_{i+1}^{n+1/2}$) at the downslope grid (i+1). However, the current grid may have multiple outflows to the downslope adjacent grid cells (Figure 1); and, meanwhile, the downslope grids may have multiple inflows coming from other upslope grid cells. In this case, the outflows at the downslope cells should be decomposed in order to predict the outflow of the current cell. The decomposition, however, is a tough challenge in theory and practice. This makes it difficult to couple the full implicit MacCormack scheme into DHSVM for overland flow routing. Nevertheless, Huang and Lee (2013) modified the full implicit MacCormack scheme to make it usable in the DEM-based overland flow

routing system, in which the flow directions are determined using the D8 algorithm. The modified MacCormack scheme in delta form for approximating the KW equations is as follows:

$$\Delta A_i^{n+1} = -\frac{\Delta t}{\Delta x}(Q_i^n - Q_{i-1}^n) + q_e \Delta t \tag{10}$$

$$(1+\frac{\lambda \Delta t}{\Delta x})\delta A_i^{n+1} = \Delta A_i^{n+1} + \frac{\lambda \Delta t}{\Delta x}\delta A_i^{n+1} \tag{11}$$

$$A_i^{n+1} = A_i^n + \delta A_i^{n+1} \tag{12}$$

The predictor step presented in the full MacCormack scheme (Eqs. 7 and 8) has been removed in the modified MacCormack scheme. Hence, we name the modified version of the MacCormack scheme as the semi-MacCormack. The semi-MacCormack algorithm can be converted to the following recursive formulas in order to implement it into DHSVM:

$$\Delta A_i^{t+\Delta t} = -\frac{\Delta t}{\Delta x}(Q_i^t - Q_{i-1}^t) + q_e \Delta t \tag{13}$$

$$(1+\frac{\lambda \Delta t}{\Delta x})\delta A_i^{t+\Delta t} = \Delta A_i^{t+\Delta t} + \frac{\lambda \Delta t}{\Delta x}(A_{i-1}^{t+\Delta t} - A_{i-1}^t) \tag{14}$$

$$A_i^{t+\Delta t} = A_i^t + \delta A_i^{t+\Delta t} \tag{15}$$

in which Q_{i-1}^t and A_{i-1}^t are, respectively, the total inflow from the up-gradient adjacent grids and the corresponding cross-sectional area at current time *t*; Q_i^t and A_i^t are, respectively, the outflow and its cross-sectional area at current grid cell *i* and time *t*; Δt and Δx are the time step and the grid size, respectively; and ΔA is the change in cross-sectional area of flow. The boundary values for the grid cells on the upstream end are assigned as zero (Wang and Hjelmfelt, 1998; Jain and Singh, 2005), i.e., $Q_u^t = 0$ and $A_u^t = 0$, where Q_u^t and A_u^t are the outflow and its cross-sectional area,

respectively, at the boundary grid cells indicated by subscript *u*.

Figure 2 presents the flow chart for routing the overland flow using the semi-MacCormack scheme in DHSVM. Specifically, the procedure consists of five main steps: (i) read initial conditions at start time; (ii) enter into the external time loop; (iii) enter into the internal spatial loop; (iv) solve the KW equations using the semi-MacCormack algorithm; (v) advance to the next time step and repeat the steps outlined above until reaching the end time. The enhanced DHSVM model is referred to as DHSVM-MacCormack.

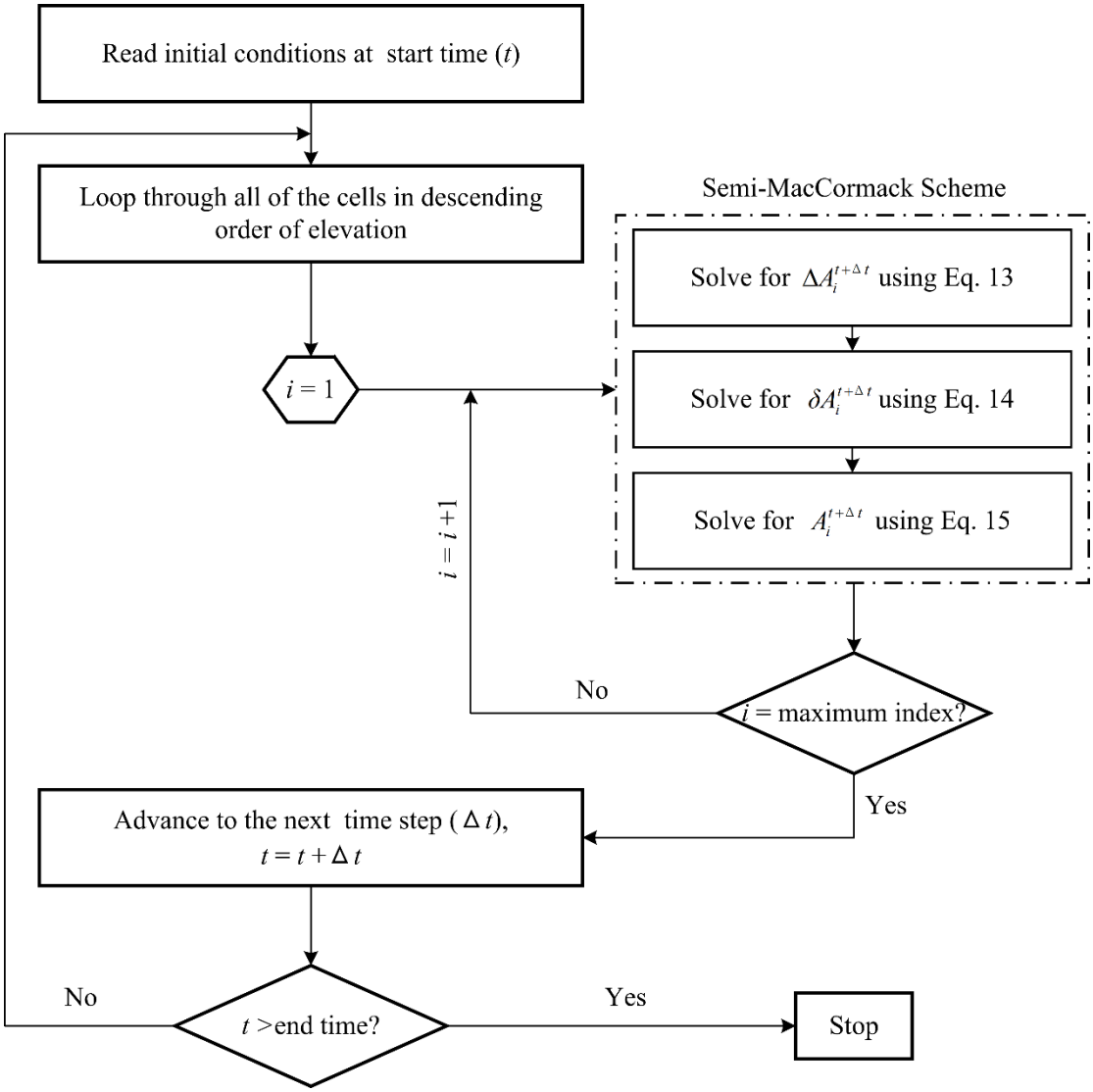

Figure 2. Flowchart for overland flow routing in DHSVM using the semi-MacCormack scheme

2.4 Numerical experiments for the MacCormack schemes

2.4.1 Experiment setup for analytical evaluation of the MacCormack schemes

An important advantage of the KW approach over the dynamic and diffusion wave approaches is that analytical solutions are possible for simple geometries (David and Michael, 1986). Eagleson (1970) provided the analytical solution for the KW overland flow with uniform rainfall. As shown in Table 1, two impermeable rectangular parking lots with different geometries are assumed to be subject to uniform rainfall with different durations and intensities. The hydrographs of flow depth at the end of the parking lots were calculated using the analytical approach, the explicit linear scheme, and the semi- and full-MacCormack schemes, respectively. The explicit linear scheme adopted in DHSVM is a commonly used FD method for solving the KW equations. Details about the KW computations with the explicit linear scheme have been documented by Chow et al. (1988). Capabilities of the numerical methods (i.e., the semi- and full-MacCormack algorithms, and the explicit linear scheme) were quantitatively assessed by using the performance indicators of the root-mean-square error (RMSE) and mean absolute error (MAE). Moreover, the CPU time requirements of different numerical methods were compared with each other. All

of the computations were run with a Lenovo notebook PC with an Intel Core i7-2620M CPU and 8 GB RAM.

Table 1 Characteristics of the synthetic overland flow cases

Test case	Parking lot geometry			Rainfall	
	Length (m)	Slope	Manning roughness coefficient	Intensity (mm/h)	Duration (s)
Case 1	182.88	0.0016	0.025	50.8	1,800
Case 2	500.00	0.0100	0.005	100.0	1,500

In the first synthetic overland flow case, the time increment (Δt) varied from 4 to 39 s for the explicit linear scheme to satisfy the CFL stability condition, and it was purposely set to 50, 100, and 150 s for the MacCormack schemes with which the stability condition is violated. The spatial step (Δx) was set to 1 m for all of the runs. The coefficient α_{mac} in Eq. (9) was calibrated to be 0.5 and 0.6 in the full- and semi-MacCormack schemes, respectively, to obtain the best fit results comparing to the analytical solution. In the second synthetic case, the time step (Δt) ranges from 0.5 to 6 s for the explicit linear scheme to satisfy the CFL stability condition, but it was increased to 10, 20, and 50 s for the MacCormack schemes for the cases against the stability condition. Likewise, the spatial step (Δx) was set to 1 m for all numerical methods, as in Case 1. The coefficient α_{mac} in Eq. (9) was best fitted to be 0.6 and 0.8 in the full- and semi-MacCormack schemes, respectively.

2.4.2 Test sites and experiment setups for numerical evaluation of DHSVM-MacCormack

The test data for DHSVM 3.1.2, which is freely available at the model's official website (http://dhsvm.pnnl.gov/), was used to test the performance of the enhanced DHSVM model (i.e., DHSVM-MacCormack). The test site, Mercer Creek watershed, is a small urban watershed near Bellevue, Washington (Figure 3). The Mercer Creek river flows through Mercer Slough and finally ends in Lake Washington (Sun et al., 2015). The watershed has a drainage area of approximately 31 km^2, and is characterized by rugged topography with elevations ranging from 16 to 326 m above sea level. The primary land use types in the watershed are urban land and conifer forest; and the predominant soil type is sandy loam soil. The 3-hourly meteorological forcing data including air temperature, wind speed, relatively humidity, precipitation, and incoming shortwave and longwave radiations at two pseudo stations are available for the test basin. They were obtained from a hydrologically consistent dataset of land surface fluxes and states for the conterminous United States that was developed by Livneh et al. (2013) based on the observations from NOAA Cooperative Observer (COOP) stations. The streamflow from the Mercer Creek watershed has been monitored by US Geological Survey station (No. 12120000; 47°36'11"N, 122°10'47"W). The streamflow records at a 15-min interval for the period from 01/01/2012-00 to 03/31/2012-21 were used for model performance assessment.

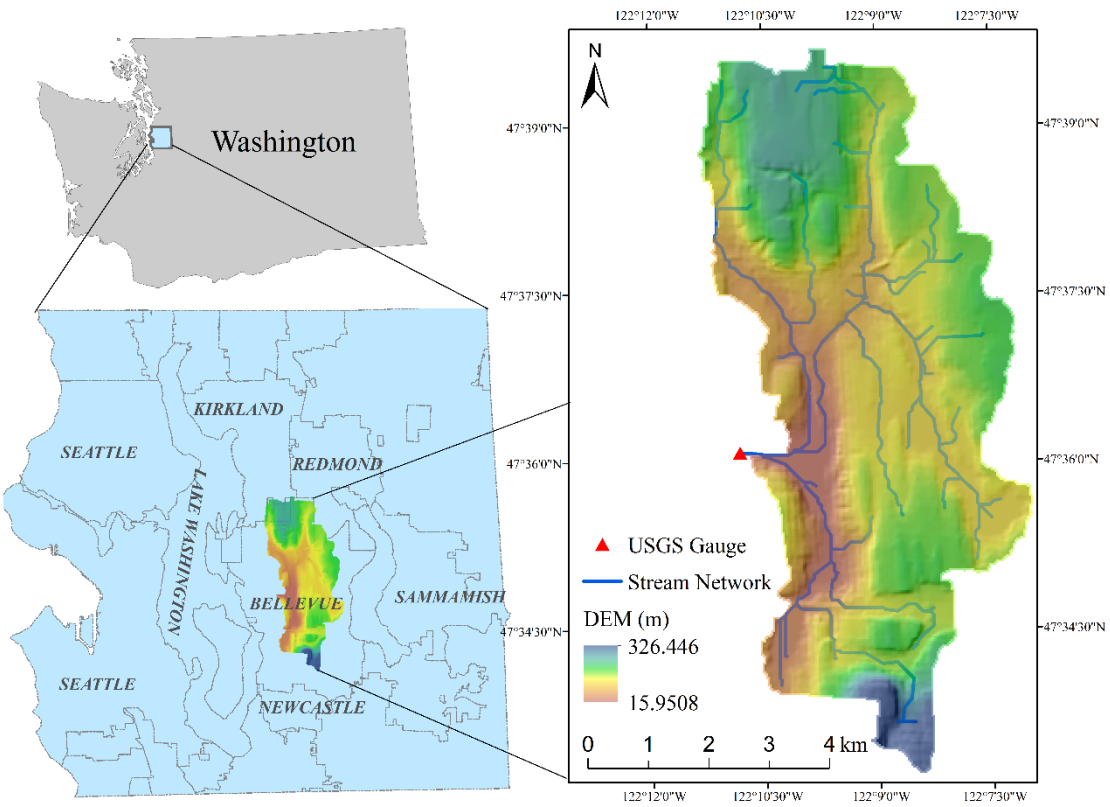

Figure 3. Map showing the location and topography of the Mercer Creek watershed

As presented in Table 2, two groups of modeling experiments were designed and carried out to assess the performance and efficiency of DHSVM-MacCormack. The modeling in the first experiment group (Exp I) was performed using the original DHSVM model (version 3.1.2), in which the KW equations are solved with the explicit linear scheme for overland flow routing. The routing time increments (Δt) are variable and updated at the beginning of each model time step to ensure they comply with the CFL stability condition at each computational grid (Chow et al., 1988). In Exp I, we set the routing option to "KINEMATIC" and the grid size to 30 m, and assigned start and end times as 01/01/2012-00 and 03/31/2012-21, respectively. The other parameters and options were kept with the default values. The simulated streamflow was quantitatively evaluated against the measurements using the (i)

Nash-Sutcliffe efficiency (NSE) coefficient (Nash and Sutcliffe, 1970) and (ii) RMSE.

Table 2 Modeling experiments for DHSVM-MacCormack

Modeling experiment	Model version	Overland flow routing method	Model time step (h)	Routing time step (s)
Exp I	DHSVM 3.1.2	KW & explicit linear	3	Variable
Exp II	DHSVM-MacCormack	KW & MacCormack	3	30, 60, 90, 120, 150, 180, 210, 240, 270, 300, 600

The second experiment group (Exp II) was undertaken with DHSVM-MacCormack, in which the KW equations are solved with the semi-MacCormack scheme. The routing time step was set to 30, 60, 90, 120, 150, 180, 210, 240, 270, 300 and 600 seconds for the purpose of testing the performance of the MacCormack algorithm. Thus, DHSVM-MacCormack was run 11 times in Exp II, with the same model parameters and configurations as in Exp I. In addition to NSE and RMSE, the relative NSE and relative RMSE, as defined in Eqs.16 and 17, were used to evaluate the simulations of Exp II against those of Exp I. Moreover, the relative CPU time, as in Eq.18, was defined to evaluate the computational efficiency of DHSVM-MacCormack in comparison to the original DHSVM model.

$$\text{Relative NSE} = 1 - \frac{\sum_{i=1}^{N}(Q_i^{\text{DHSVM3.1.2}} - Q_i^{\text{DHSVM-MacCormack}})^2}{\sum_{i=1}^{N}(Q_i^{\text{DHSVM3.1.2}} - Q_m^{\text{DHSVM3.1.2}})^2} \quad (16)$$

$$\text{Relative RMSE} = \sqrt{\frac{1}{N}\sum_{i=1}^{N}(Q_i^{\text{DHSVM-MacCormack}} - Q_i^{\text{DHSVM3.1.2}})^2} \quad (17)$$

$$\text{Relative CPU time} = \frac{(\text{CPU time})^{\text{DHSVM-MacCormack}}}{(\text{CPU time})^{\text{DHSVM3.1.2}}} \quad (18)$$

where N is the total number of time steps during the simulation period; Q_i is the simulated streamflow at the time step i; and Q_m is the mean value of the simulated streamflow.

The test site, Mercer Creek (MC) watershed, is relatively small. To assess impacts of watershed sizes on the computational time with the MacCormack scheme, DHSVM-MacCormack is also applied to a large watershed. This larger watershed is the upper Heihe River Basin (UHRB) with a drainage area of about 100,09 km^2, as shown in Table 3, in northwest China. More details about this watershed is available in Zhang et al. (2016). The grid size, routing time step and simulation length were consistently set as 150 m, 600 s and 3 months, respectively, for both the small and large watersheds. The computational environment and model settings were kept the same for the different cases as listed in Table 3. Moreover, impacts of different modeling grid sizes (e.g., 30, 45, 60, 90 and 150 m) on the computational time with the original and enhanced DHSVM (i.e., DHSVM-MacCormack) models were investigated using the Mercer Creek watershed.

Table 3 Applications of DHSVM-MacCormack to two catchments with different sizes

Catchment	Catchment size (km^2)	Simulation length (months)	Grid size (m)/routing time step (s)
Mercer Creek watershed	31	3	150/600

Upper Heihe River Basin (UHRB)	10,009	3	150/600

3 Results and discussion

3.1 Analytical verification

Figure 4 presents the numerical results and analytical solution for the first synthetic overland flow case (Table 1). The flow depth time series produced by the MacCormack and explicit linear schemes match the analytical solution very well, although there are some small differences at the crest. This indicates that both the full-MacCormack and semi-MacCormack algorithms can work very well and are comparable to the explicit linear scheme in terms of simulation accuracy even when the time step does not satisfy the stability condition. Thus, the MacCormack approaches can relax the restriction on temporal and spatial intervals imposed by the CFL stability condition. When the time step is 150 s, the computational times of the full- and semi-MacCormack schemes was 0.006 and 0.003 s, respectively, which are about 7-15 times faster than that of the explicit linear scheme (0.046 s). Therefore, the MacCormack schemes can save the computation time considerably, compared to the explicit linear method. The RMSEs and MAEs are very small for all of the numerical methods, as indicated and summarized in Table 4, which confirms their reliability for solving the KW equations. The accuracy tends to decrease with increasing time steps for both the full- and semi-MacCormack schemes. Moreover, with a same time step,

the full-MacCormack scheme performs slightly better than the semi-MacCormack scheme, particularly for the recession limb of the hydrograph. This is reasonable since the predictor step of the full-MacCormack scheme has been removed in the semi-MacCormack scheme.

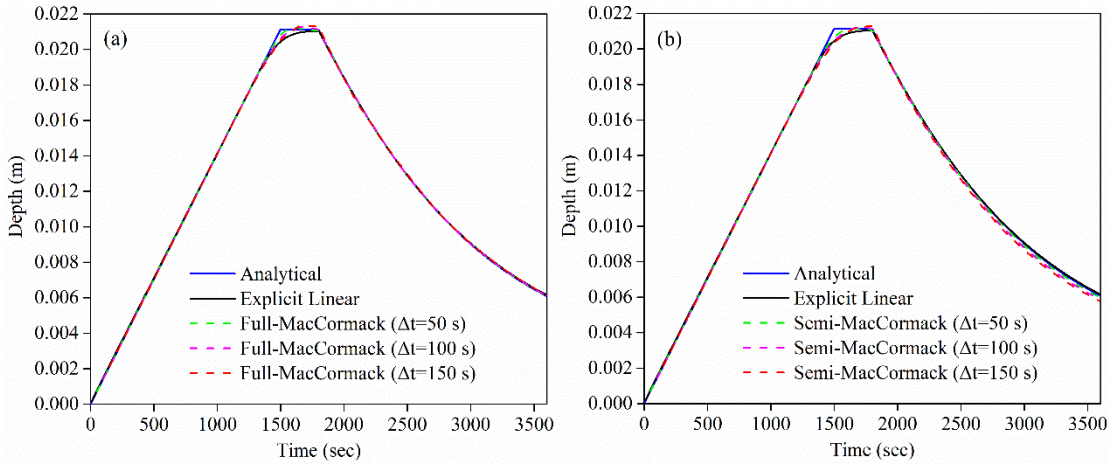

Figure 4. Flow depth time series for Case 1 estimated using the full-MacCormack (left) and semi-MacCormack (right) schemes

Table 4 A summary of performance of the numerical methods for synthetic overland flow cases

Test case	Numerical scheme	Time step (Δt, s)	RMSE (m)	MAE (m)	CPU time (s)
Case 1	Explicit linear	4-39	1.37×10^{-4}	7.88×10^{-5}	0.046
	Full-MacCormack	50	4.26×10^{-5}	1.40×10^{-5}	0.018
		100	8.88×10^{-5}	3.78×10^{-5}	0.010
		150	1.38×10^{-4}	6.97×10^{-5}	0.006
	Semi-MacCormack	50	9.19×10^{-5}	5.97×10^{-5}	0.009
		100	1.79×10^{-4}	1.25×10^{-4}	0.004
		150	2.68×10^{-4}	1.94×10^{-4}	0.003
Case 2	Explicit linear	0.5-6	3.23×10^{-5}	1.85×10^{-5}	1.090
	Full-MacCormack	10	1.12×10^{-5}	2.46×10^{-6}	0.406

		20	2.27×10^{-5}	6.61×10^{-6}	0.186
		50	5.36×10^{-5}	2.52×10^{-5}	0.073
		10	3.17×10^{-5}	1.21×10^{-5}	0.184
	Semi-MacCormack	20	5.49×10^{-5}	2.19×10^{-5}	0.092
		50	1.05×10^{-4}	4.66×10^{-5}	0.034

Figure 5 shows the results of Case 2. The full-MacCormack scheme induces some small oscillations before reaching the equilibrium, while the semi-MacCormack scheme is lagged to reach the maximum flow depth. Despite of these discrepancies, the time series obtained by both MacCormack schemes are very close to the analytical solution, as well as to that simulated by the explicit linear scheme. As shown in Table 4, all of the numerical approaches can produce good overland flow simulations for Case 2, with very small RMSEs and MAEs. Similar to Case 1, the full-MacCormack scheme slightly outperforms the semi-MacCormack method when a same time step is employed, although it requires slightly more computational time. Results in Figure 5 clearly demonstrated that both the full- and semi-MacCormack schemes are more computationally efficient than the explicit linear scheme while achieving a similar accuracy.

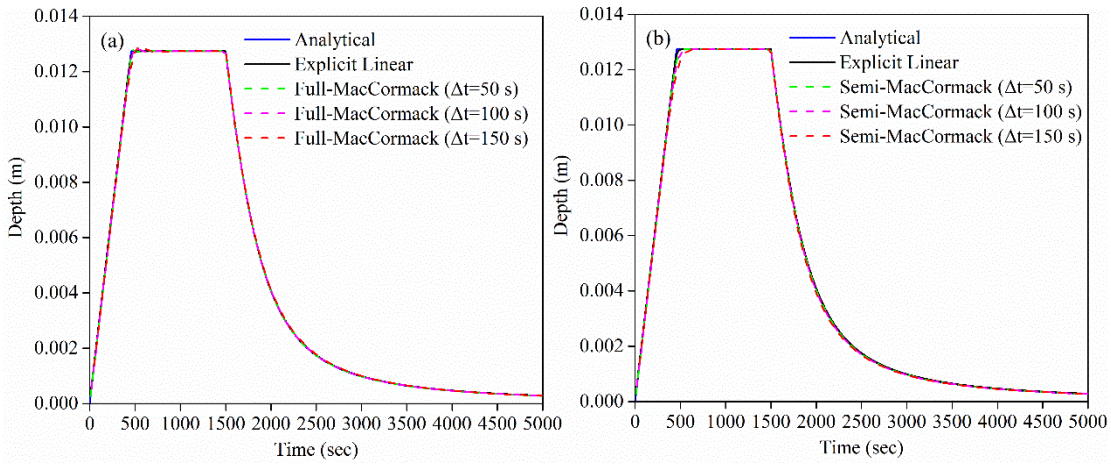

Figure 5. Flow depth time series for Case 2 estimated using the full-MacCormack (left) and semi-MacCormack (right) schemes

3.2 Evaluation of DHSVM-MacCormack

Figure 6 presents daily and sub-daily (3 hourly) streamflow observations and the simulations obtained from the two groups of modeling experiments (i.e., Exps I and II) at the outlet of the Mercer Creek watershed for the period from January 1, 2012 to March 31, 2012. In Exp I, the original DHSVM model simulated a streamflow hydrograph that exhibits a reasonably good match with the observed one. The corresponding NSE and RMSE are 0.7852 and 0.3625 m^3/s, respectively, for daily streamflow, and 0.6163 and 0.5757 m^3/s, respectively, for sub-daily streamflow (Table 5). The results indicate a good applicability of the original DHSVM model to the Mercer Creek watershed according to the model evaluation guidelines proposed by Moriasi et al. (2007). However, it takes a quite large CPU time of about one day and a half (35.50 h) to complete Exp I due to low computational efficiency of routing the overland flow. The considerable computational time requirement by the explicit linear

scheme in the original DHSVM model significantly restricts the practicality of DHSVM's applications with the KW option for overland flow routing. The computational cost would become much worse when a longer-term, higher-resolution hydrological simulation is needed for a larger watershed.

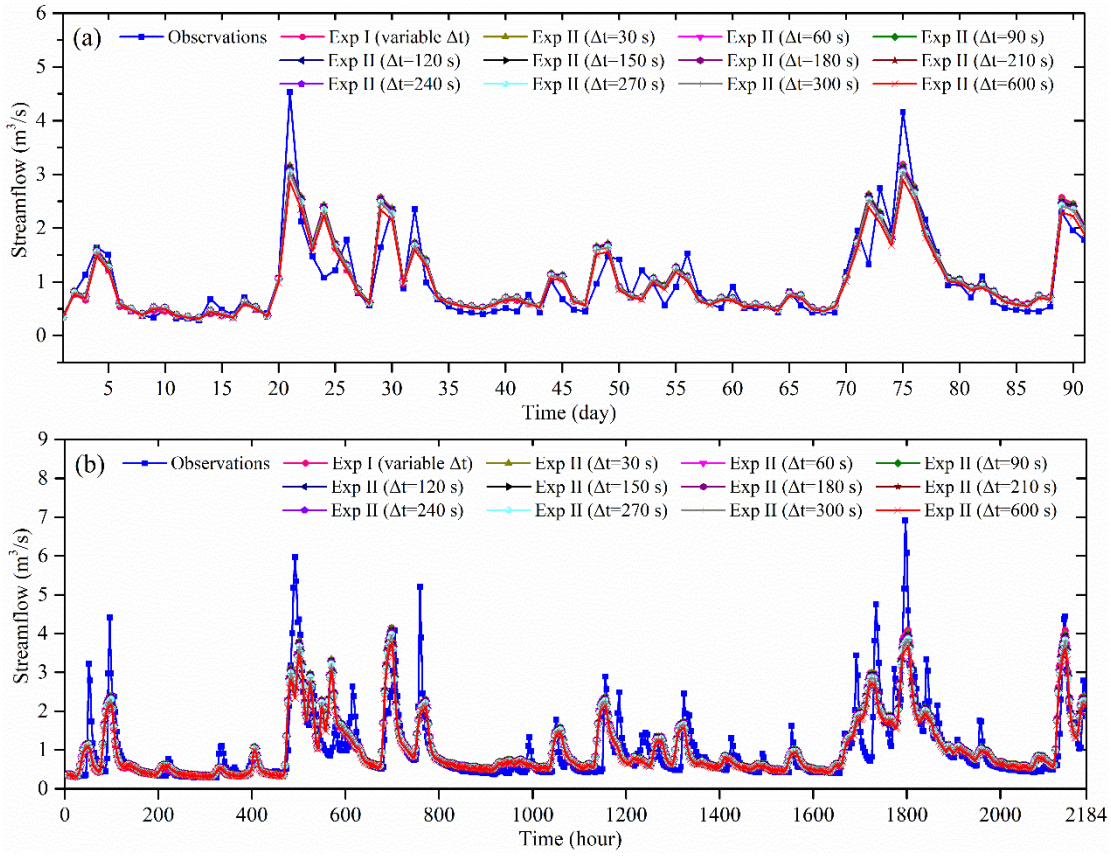

Figure 6. Comparison of daily (a) and sub-daily (b) streamflow observations with the simulations generated from the two groups of modeling experiments for the Mercer Creek watershed from January 1, 2012 through March 31, 2012

Table 5 Comparison of experiment results in terms of simulation accuracy of daily and sub-daily (in parentheses) streamflow and computational efficiency

Modeling experiment	Routing time step (s)	NSE	Relative NSE	RMSE (m^3/s)	Relative RMSE	CPU time (h)	Relative CPU time
Exp I	Variable	0.7852 (0.6163)	1.0000 (1.0000)	0.3625 (0.5757)	0.0000 (0.0000)	35.50	1.0000
Exp II	30	0.7833 (0.6186)	0.9962 (0.9965)	0.3641 (0.5740)	0.0437 (0.0476)	3.37	0.0949
	60	0.7849 (0.6201)	0.9969 (0.9969)	0.3628 (0.5729)	0.0398 (0.0442)	1.70	0.0479
	90	0.7861 (0.6213)	0.9973 (0.9972)	0.3618 (0.5719)	0.0372 (0.0422)	1.19	0.0335
	120	0.7870 (0.6223)	0.9975 (0.9973)	0.3610 (0.5712)	0.0358 (0.0414)	0.86	0.0242
	150	0.7878 (0.6231)	0.9975 (0.9973)	0.3603 (0.5706)	0.0354 (0.0415)	0.70	0.0197
	180	0.7885 (0.6238)	0.9974 (0.9972)	0.3597 (0.5701)	0.0359 (0.0425)	0.64	0.0180
	210	0.7891 (0.6250)	0.9972 (0.9969)	0.3592 (0.5692)	0.0377 (0.0448)	0.50	0.0141
	240	0.7895 (0.6249)	0.9970 (0.9966)	0.3589 (0.5693)	0.0391 (0.0463)	0.45	0.0127
	270	0.7898 (0.6253)	0.9966 (0.9962)	0.3586 (0.5690)	0.0415 (0.0489)	0.40	0.0113
	300	0.7901 (0.6256)	0.9961 (0.9958)	0.3584 (0.5687)	0.0444 (0.0520)	0.37	0.0104
	600	0.7865 (0.6270)	0.9833 (0.9837)	0.3615 (0.5676)	0.0919 (0.1020)	0.20	0.0056

Simulated streamflow hydrographs from Exp. II with the enhanced DHSVM model (i.e., DHSVM-MacCormack) produced almost exactly the same results as those from Exp I (i.e., results overlapped on each other) when the routing time step (Δt) is less than 300 s (Figure 6). Only very small differences between Exps I and II can be discerned when Δt is increased to 300 and 600 s. As shown in Table 5, the NSEs and RMSEs of daily streamflow vary from 0.7833 to 0.7901, and from 0.3584 to 0.3641 m^3/s, respectively, with different routing time steps in Exp II, which are comparable to those of Exp I (0.7852 and 0.3625 m^3/s). Using results from Exp I as the baseline, the relative NSEs and relative RMSEs span from 0.9833 to 0.9975, and from 0.0354 to 0.0919, respectively, for daily streamflow; and 0.9837~0.9973 and 0.0414~0.1020, respectively, for the sub-daily streamflow. Such high relative NSEs together with the low relative RMSEs clearly indicate the comparable performance between the explicit linear scheme with DHSVM and the semi-MacCormack scheme with DHSVM-MacCormack. The narrow spans of the NSEs and RMSEs in Exp II show that the semi-MacCormack scheme still has space to further reduce the computation time without much compromise of the accuracy by using a larger time step. Specifically, the required CPU time, which decreases with increasing time intervals, is observed to be in the range of 0.20-3.37 h in Exp II, in stark contrast to 35.50 h in Exp I. The relative CPU time of Exp II ranges from 0.0949 to 0.0056 which is remarkably shorter than 1.0 from Exp I. These results again indicate that DHSVM-MacCormack can significantly improve the computational efficiency while obtaining almost the same simulation accuracy as that from the original DHSVM

model. In our experiment, the computational time of the original DHSVM model is about one day and a half (35.50 h) for a simulation period of three months. However, it can be cut down to several dozen minutes by using DHSVM-MacCormack instead without losing noticeable simulation accuracy.

From Table 5, it is seen that the streamflow simulation accuracy in Exp II tends to improve slightly when the routing time steps become larger (30-300 s). This seems inconsistent with the finding of the analytical verification, i.e., the accuracy decreases as the time step increases. The seeming contradiction can be well explained by the differences between the observed and model simulated streamflow. Based on the model default parameters, the streamflow was actually slightly overestimated for the baseflow. Thus, the error introduced by the increase of computational time compensates the one caused by the model default parameters. More specifically, the overestimation of streamflow would be ameliorated with increasing routing time steps in the semi-MacCormack scheme, since overland flow tends to be underestimated gradually as revealed in the analytical verification. As a result, the streamflow simulation accuracy gets improved before reaching a turning point, which is observed when the routing time step reaches 600 s. From that point, the underestimated volume of overland flow, resulting from the coarsening routing time step, begins to exceed the overestimated volume of streamflow.

Impacts of watershed sizes on the computational time using the MacCormack scheme are investigated by applying DHSVM-MacCormack to a much larger watershed, the UHRB in China. With the same model setup as listed in Table 3,

simulation results show that the computational time required by DHSVM-MacCormack were 0.01 hour and 3.35 hour, respectively, in modelling the Mercer Creek watershed and the UHRB. In contrast, it took the original DHSVM model 0.03 hour and over two weeks, respectively, for these two watersheds. Although the required computational time for either DHSVM or DHSVM-MacCormack appear to be proportional to the watershed size, the advantage of the MacCormack scheme on the reduction of computational time is more significant with the larger watershed (i.e., Heihe watershed). In particular, the computation time required by the original DHSVM model increased by more than 11,200-fold when the watershed size is increased only by about 322 times. But for the DHSVM-MacCormack model, the increase in the computation time is only about 335 times. Such results indicate that the improvement on the computational efficiency of overland flow MacCormack routing scheme is significantly more when the MacCormack scheme is applied to a larger watershed with a constant grid size.

To assess impacts of different modeling grid sizes on the computation time, we have carried out a series of different simulations with grid sizes being at 30, 45, 60, 90 and 150 m, respectively, using both the original and enhanced DHSVM models with the Mercer Creek watershed. In these simulations, the computational environment and model settings were kept the same except for the modeling grid sizes. Figure 7 shows that the computational time required by the original DHSVM model decreases from 35.5 to 0.03 hours when the grid size increases from 30 to 150 m whereas the computational time required by DHSVM-MacCormack reduces from 0.2 to 0.01

hours. This clearly demonstrates that the computational time with the MacCormack scheme decreases when the grid size increases for a given basin. The reduction is more obvious for the original DHSVM model than for DHSVM-MacCormack as expected since the latter is already very effective when the modeling grid size is small for a given large watershed.

These results illustrate that the computational time of the MacCormack scheme depend on the size of both the basin and the modeling grid cell. For applications to larger river basins, the demand for computational time can be compensated by increasing grid sizes. Thus, selecting an appropriate grid cell size that is as large as possible while satisfying the accuracy requirement is the key to reduce computational time when applying MacCormack scheme to a large watershed. From a practice point of view, one can also use the MacCormack scheme in conjunction with HPC or parallel and distributed computations (Li et al., 2011; Vivoni et al., 2011) for conducting the routing for a very large river basin.

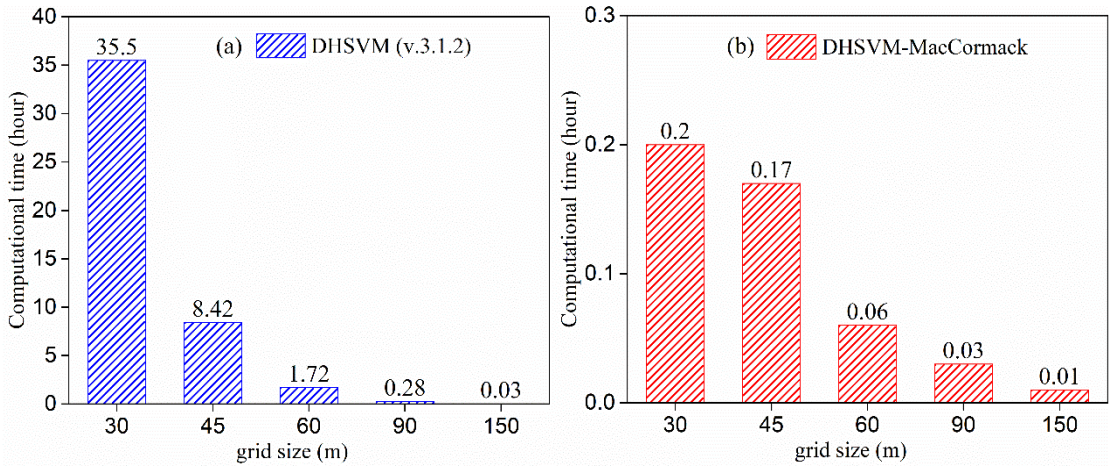

Figure 7. Computational time required by DHSVM (a) and DHSVM-MacCormack (b) for the Mercer Creek watershed with different grid sizes

In this study only the semi-MacCormack scheme was implemented in DHSVM for the overland flow routing. The full version of the MacCormack scheme (full-MacCormack), however, proved to outperform the semi-MacCormack in terms of simulation accuracy, although the latter is slightly more computationally efficient, as presented in Section 3.1. Thus, in a follow-up study, we expect to apply the full-MacCormack scheme to overland flow routing in PDHMs, despite of the aforementioned theoretical and practical challenges. In the version of 3.1.2, flow paths are determined by the D4 algorithm, which complicates the integration of the full-MacCormack algorithm into DHSVM, because each computational grid may have multiple inflows and outflows. However, the coupling of the full-MacCormack scheme for watershed routing may become more plausible for other PHDMs with the D8 algorithm determining flow directions, since each computational grid has only one outflow in spite of possible multiple inflows.

4 Conclusions

This study applied, for the first time, the MacCormack numerical scheme to overland flow routing in DHSVM, a representative high-spatial resolution, process-based, distributed hydrological model. The MacCormack scheme proved to be applicable and efficient when coupled with DHSVM. After verifying against the analytical solutions for two synthetic overland flow cases with uniform rainfall, the semi-MacCormack algorithm was then implemented into DHSVM to solve the kinematic equations for overland flow routing. The performance and practicability of

the enhanced DHSVM model (i.e., DHSVM-MacCormack) were assessed by performing two groups of modeling experiments (i.e., Exp I and Exp II) over the Mercer Creek watershed.

The analytical verification indicated that both the semi and full versions of the MacCormack schemes (i.e., semi-MacCormack and full-MacCormack) exhibit robust numerical stability even with large time steps that violates the CFL stability condition. They were demonstrated to be significantly more computationally efficient than the explicit linear scheme. Additionally, despite more time-consuming when a same time step is employed, the full-MacCormack scheme slightly outperformed the semi-version in terms of simulation precision, especially for the falling limb of the hydrographs.

The two groups of modelling experiments in the Mercer Creek watershed show that DHSVM-MacCormack can considerably improve the computational efficiency while preserving the same simulation accuracy of the original DHSVM model. With the same computational environment and model settings, DHSVM-MacCormack can reduce the CPU time from about one day and a half, required by the original DHSVM model, to several dozen minutes for a simulation period of three months (January 1, 2012 to March 31, 2012), without any noticeable sacrifice of the accuracy.

In addition, our results show that the reduction of computational time is significantly more with the larger watershed (i.e., Heihe watershed vs. Mercer Creek watershed) using DHSVM-MacCormack than DHSVM, although the required computational time for both DHSVM and DHSVM-MacCormack appear to be

proportional to the watershed size. Furthermore, our results show that the computational efficiency of applying the MacCormack scheme depend both on the sizes of the watershed and the grid cell. Thus, selecting an appropriate grid cell size that is as large as possible while satisfying the accuracy requirement can be a key to have a maximum reduction of the computational time. The MacCormack scheme shows promise for applications to watershed routing in high spatial resolution PDHMs in light of its outstanding computational efficiency. Future work will focus on implementing the full-MacCormack scheme to PDHM with the D8 algorithm determining flow directions.

Acknowledgments

This study was financially supported by the National Key R&D Program of China (2017YFA0603603) and National Natural Science Foundation of China (No. 91425303 and No. 41671373). It is also partially supported by the United States Department of Transportation through award #OASRTRS-14-H-PIT to the University of Pittsburgh, the William Kepler Whiteford Professorship from the University of Pittsburgh, and the Qinglan Talent Program of Nanjing Normal University, China. The authors would like to thank the UW Hydro Computational Hydrology group at the University of Washington (http://uw-hydro.github.io/) for providing source codes and test site data of DHSVM. The authors also thank Prof. Jeen-Shang Lin for polishing the language of our paper, and Dr. Ning Sun for her kind help in this research. The careful reviews and constructive comments of the three anonymous referees are

greatly appreciated.

References

Akan, A.O., Houghtalen, R.J., 2003. Urban hydrology, hydraulics, and stormwater quality: engineering applications and computer modeling. John Wiley & Sons.

Alvarenga, L.A., de Mello, C.R., Colombo, A., Cuartas, L.A., Bowling, L.C., 2016. Assessment of land cover change on the hydrology of a Brazilian headwater watershed using the Distributed Hydrology-Soil-Vegetation Model. CATENA 143: 7-17. http://dx.doi.org/10.1016/j.catena.2016.04.001

Beven, K.J., 2011. Rainfall-runoff modelling: the primer. John Wiley & Sons.

Chow, V.T., Maidment, D.R., Mays, L.W., 1988. Applied hydrology. McGraw-Hill, New York.

Costa-Cabral, M.C., Burges, S.J., 1994. Digital Elevation Model Networks (DEMON): A model of flow over hillslopes for computation of contributing and dispersal areas. Water Resour. Res. 30(6): 1681-1692. http://dx.doi.org/10.1029/93WR03512

Cuo, L., Lettenmaier, D.P., Alberti, M., Richey, J.E., 2009. Effects of a century of land cover and climate change on the hydrology of the Puget Sound basin. Hydrol. Process. 23(6): 907-933. http://dx.doi.org/10.1002/hyp.7228

Cuo, L., Lettenmaier, D.P., Mattheussen, B.V., Storck, P., Wiley, M., 2008. Hydrologic prediction for urban watersheds with the Distributed Hydrology-Soil-Vegetation Model. Hydrol. Process. 22(21): 4205-4213.

David, S., Michael, E.M., 1986. Kinematic hydrology and modelling. Developments in Water Science. Elsevier, 23-42 pp. DOI:http://dx.doi.org/10.1016/S0167-5648(08)70017-0

Dickerson-Lange, S.E., Mitchell, R., 2014. Modeling the effects of climate change projections on streamflow in the Nooksack River basin, Northwest Washington. Hydrol. Process. 28(20): 5236-5250. http://dx.doi.org/10.1002/hyp.10012

Doten, C.O., Bowling, L.C., Lanini, J.S., Maurer, E.P., Lettenmaier, D.P., 2006. A spatially distributed model for the dynamic prediction of sediment erosion and transport in mountainous forested watersheds. Water Resour. Res. 42(4). http://dx.doi.org/10.1029/2004WR003829

Du, J., Xie, S., Xu, Y., Xu, C.-y., Singh, V.P., 2007. Development and testing of a simple physically-based distributed rainfall-runoff model for storm runoff simulation in humid forested basins. J. Hydrol. 336(3–4): 334-346. http://dx.doi.org/10.1016/j.jhydrol.2007.01.015

Eagleson, P.S., 1970. Dynamic Hydrology McGraw-Hill, New York.

Fatichi, S. et al., 2016. An overview of current applications, challenges, and future trends in distributed process-based models in hydrology. Journal of Hydrology 537: 45-60.

Fenicia, F., Kavetski, D., Savenije, H.H.G., Pfister, L., 2016. From spatially variable streamflow to distributed hydrological models: Analysis of key modeling decisions. Water Resour. Res. 52(2): 954-989. http://dx.doi.org/10.1002/2015WR017398

Furst, J., Furmanek, P., 2011. An implicit MacCormack scheme for unsteady flow calculations. Comput. Fluids 46(1): 231-236. http://dx.doi.org/10.1016/j.compfluid.2010.09.036

Huang, P.-C., Lee, K.T., 2013. An efficient method for DEM-based overland flow routing. J. Hydrol. 489: 238-245. http://dx.doi.org/10.1016/j.jhydrol.2013.03.014

Jain, M.K., Singh, V.P., 2005. DEM-based modelling of surface runoff using diffusion wave equation. J. Hydrol. 302(1–4): 107-126. http://dx.doi.org/10.1016/j.jhydrol.2004.06.042

Kazezyılmaz-Alhan, C.M., Medina Jr, M.A., Rao, P., 2005. On numerical modeling of overland flow. Appl. Math. Comput. 166(3): 724-740. http://dx.doi.org/10.1016/j.amc.2004.06.063

Lanini, J.S., Clark, E.A., Lettenmaier, D.P., 2009. Effects of fire-precipitation timing and regime on post-fire sediment delivery in Pacific Northwest forests. Geophys. Res. Lett. 36. http://dx.doi.org/10.1029/2008GL034588

Li, T., Wang, G., Chen, J., Wang, H., 2011. Dynamic parallelization of hydrological model simulations. Environmental Modelling & Software 26(12): 1736-1746. http://dx.doi.org/https://doi.org/10.1016/j.envsoft.2011.07.015

Lighthill, M.J., Whitham, G.B., 1955. On Kinematic Waves. I. Flood Movement in Long Rivers. Proceedings of the Royal Society of London. Series A. Mathematical and Physical Sciences 229(1178): 281-316. http://dx.doi.org/10.1098/rspa.1955.0088

Livneh, B., Rosenberg, E.A., Lin, C., Nijssen, B., Mishra, V., Andreadis, K.M.,

Maurer, E.P., Lettenmaier, D.P., 2013. A Long-Term Hydrologically Based Dataset of Land Surface Fluxes and States for the Conterminous United States: Update and Extensions. J. Climate 26(23): 9384-9392.

MacCormack, R., 2003. The Effect of Viscosity in Hypervelocity Impact Cratering. J. Spacecraft and Rockets 40(5): 757-763. http://dx.doi.org/10.2514/2.6901

MacCormack, R.W., 1982. A numerical method for solving the equations of compressible viscous flow. AIAA J. 20(9): 1275-1281.

Miller, J.E., 1984. Basic concepts of kinematic-wave models. U.S. Geological Survey Professional Paper 1302. Washington, DC: U.S. Government Printing Office.

Moriasi, D.N., Arnold, J.G., Van Liew, M.W., Bingner, R.L., Harmel, R.D., Veith, T.L., 2007. Model evaluation guidelines for systematic quantification of accuracy in watershed simulations. T. ASABE 50(3): 885-900.

Nash, J.E., Sutcliffe, J.V., 1970. River flow forecasting through conceptual models part I — A discussion of principles. J. Hydrol. 10(3): 282-290. http://dx.doi.org/10.1016/0022-1694(70)90255-6

Ochoa-Rodriguez, S. et al., 2015. Impact of spatial and temporal resolution of rainfall inputs on urban hydrodynamic modelling outputs: A multi-catchment investigation. J. Hydrol. 531: 389-407.

Paniconi, C., Putti, M., 2015. Physically based modeling in catchment hydrology at 50: Survey and outlook. Water Resour. Res. 51(9): 7090-7129.

Schulla, J., Jasper, K., 2007. Model description wasim-eth, Institute for Atmospheric and Climate Science, Swiss Federal Institute of Technology, Zürich.

Storck, P., Bowling, L., Wetherbee, P., Lettenmaier, D., 1998. Application of a GIS-based distributed hydrology model for prediction of forest harvest effects on peak stream flow in the Pacific Northwest. Hydrol. Process. 12(6): 889-904.

Sun, N., Yearsley, J., Voisin, N., Lettenmaier, D.P., 2015. A spatially distributed model for the assessment of land use impacts on stream temperature in small urban watersheds. Hydrol. Process. 29(10): 2331-2345.

Thanapakpawin, P., Richey, J., Thomas, D., Rodda, S., Campbell, B., Logsdon, M., 2007. Effects of landuse change on the hydrologic regime of the Mae Chaem river basin, NW Thailand. J. Hydrol. 334(1–2): 215-230. http://dx.doi.org/10.1016/j.jhydrol.2006.10.012

Tsai, T.-L., Yang, J.-C., 2005. Kinematic wave modeling of overland flow using characteristics method with cubic-spline interpolation. Adv. Water Res. 28(7): 661-670. http://dx.doi.org/10.1016/j.advwatres.2005.01.005

Tseng, M.H., 2010. Kinematic wave computation using an efficient implicit method. J. Hydrodyn. 12(3): 329-338.

Vivoni, E.R., Mascaro, G., Mniszewski, S., Fasel, P., Springer, E.P., Ivanov, V.Y., Bras, R.L., 2011. Real-world hydrologic assessment of a fully-distributed hydrological model in a parallel computing environment. J. Hydrol. 409(1): 483-496. http://dx.doi.org/https://doi.org/10.1016/j.jhydrol.2011.08.053

Wang, M., Hjelmfelt, A., 1998. DEM Based Overland Flow Routing Model. Journal of Hydrologic Engineering 3(1): 1-8. http://dx.doi.org/10.1061/(ASCE)1084-0699(1998)3:1(1)

Wigmosta, M.S., Perkins, W.A., 2001. Simulating the effects of forest roads on watershed hydrology, Land Use and Watersheds: Human Influence on Hydrology and Geomorphology in Urban and Forest Areas. American Geophysical Union.

Wigmosta, M.S., Vail, L.W., Lettenmaier, D.P., 1994. A distributed hydrology-vegetation model for complex terrain. Water Resour. Res. 30(6): 1665-1679.

Wong, T.S.W., 2011. Overland flow and surface runoff. Hydrological Science and Engineering. Nova Science Publishers Inc, New York, United States.

Yang, D., 1998. Distributed hydrologic model using hillslope discretization based on catchment area function: Development and applications. Tokyo, Japan: University of Tokyo.

Yu, C., Duan, J.G., 2014. High resolution numerical schemes for solving kinematic wave equation. J. Hydrol. 519, Part A: 823-832. http://dx.doi.org/10.1016/j.jhydrol.2014.08.003

Zhang, L., Nan, Z., Xu, Y., Li, S., 2016. Hydrological Impacts of Land Use Change and Climate Variability in the Headwater Region of the Heihe River Basin, Northwest China. PLoS ONE 11(6): e0158394. http://dx.doi.org/10.1371/journal.pone.0158394

Figure 1

Click here to download high resolution image

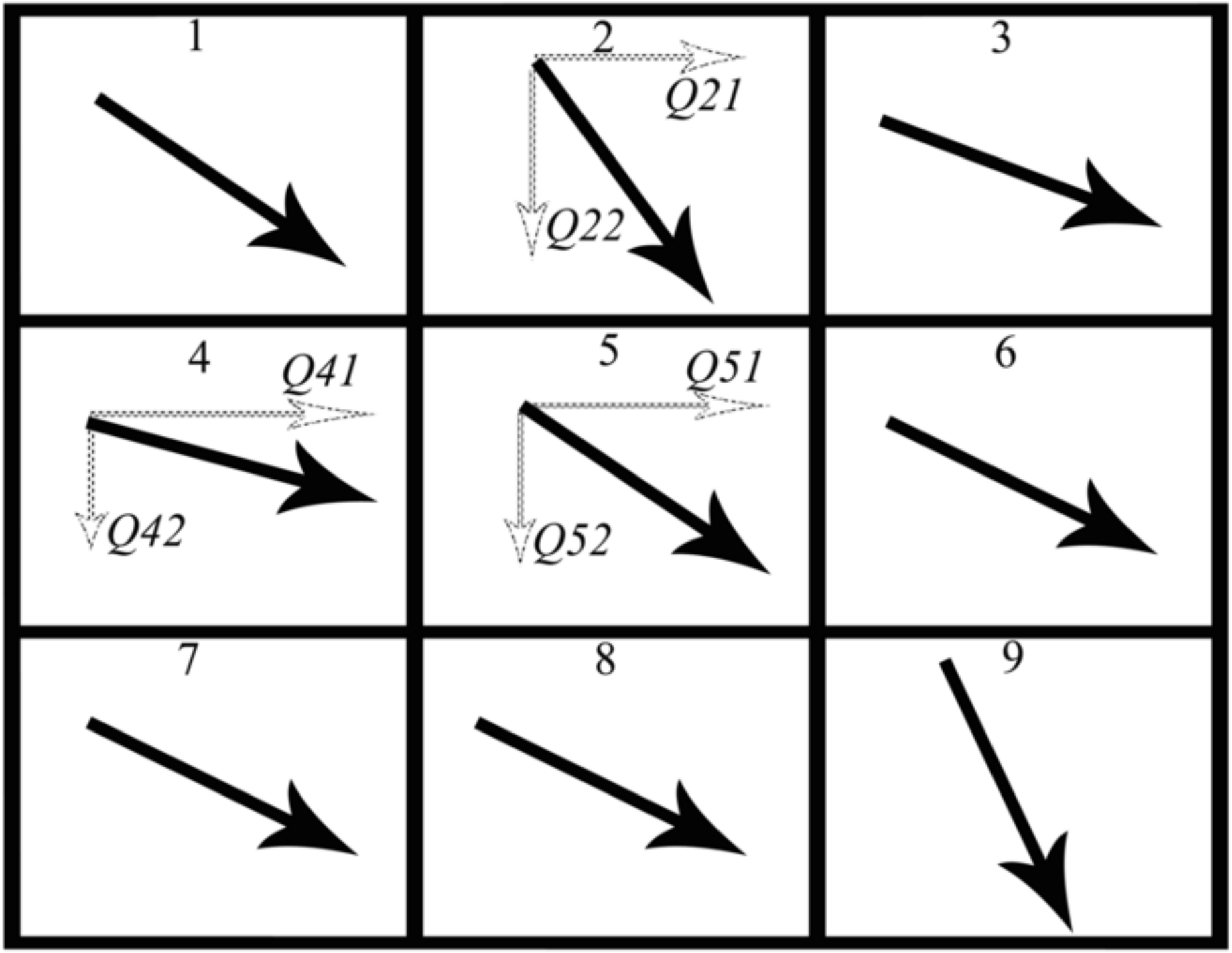

Figure 2
Click here to download high resolution image

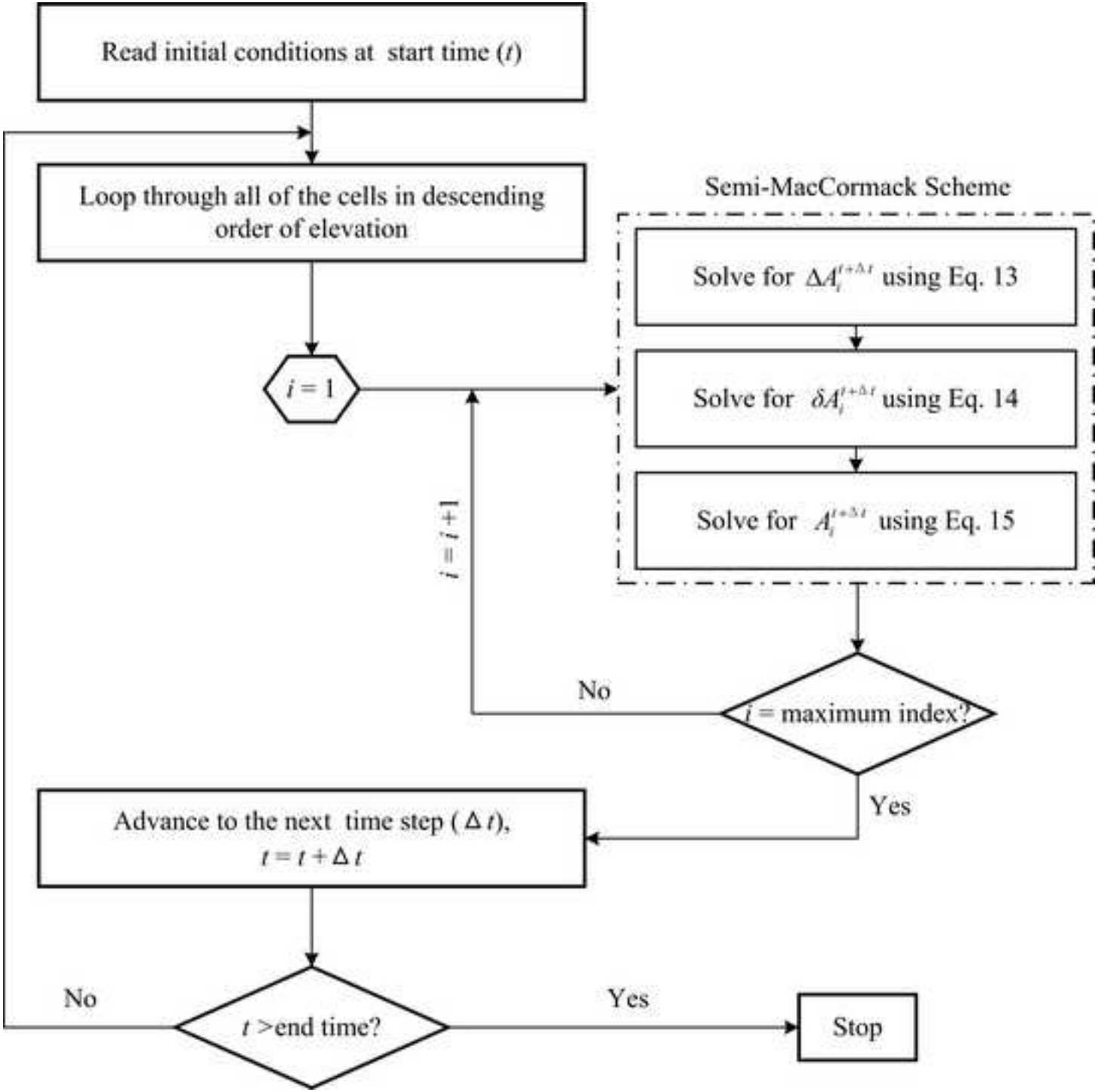

Figure 3
Click here to download high resolution image

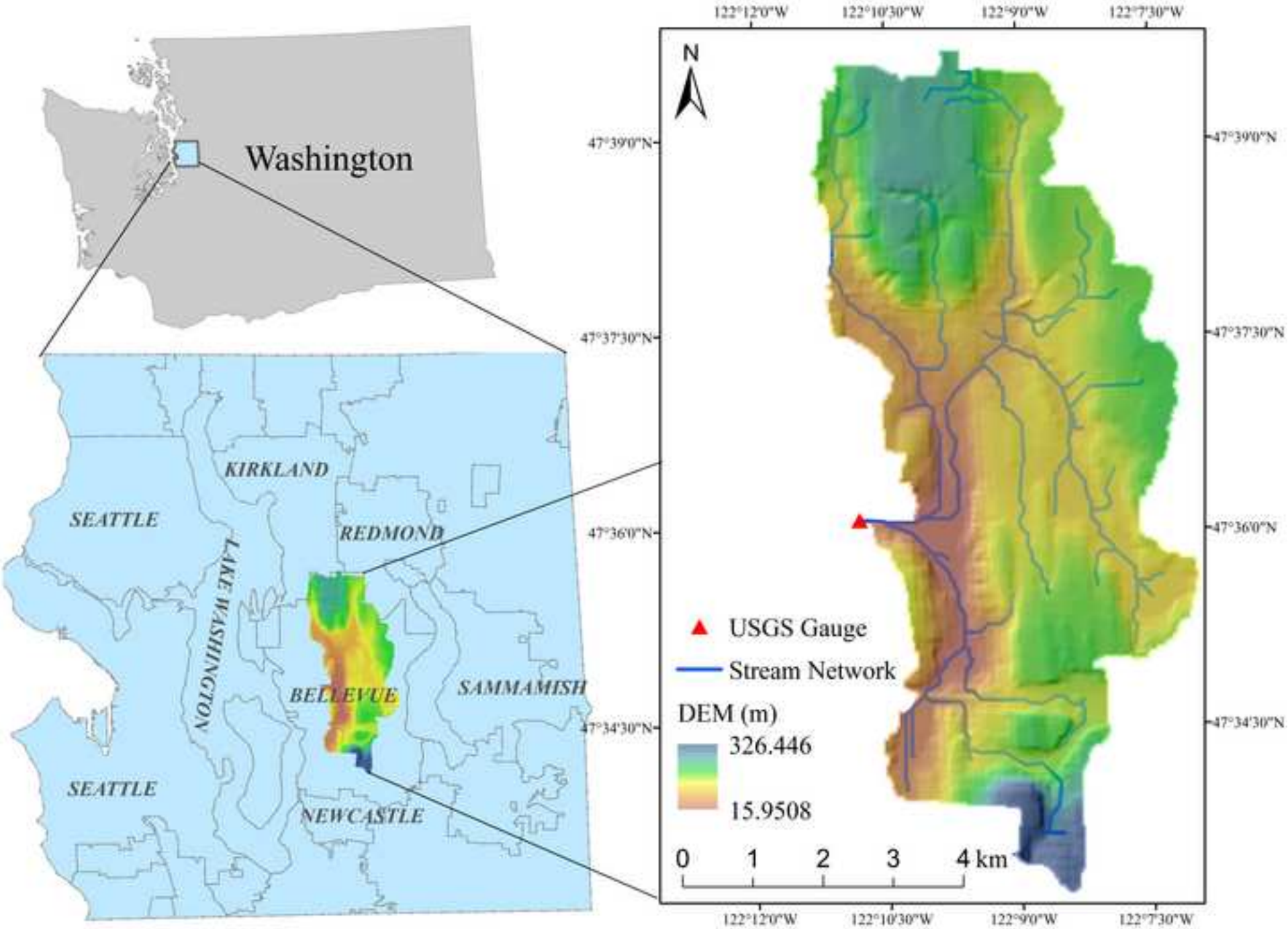

Figure 4
Click here to download high resolution image

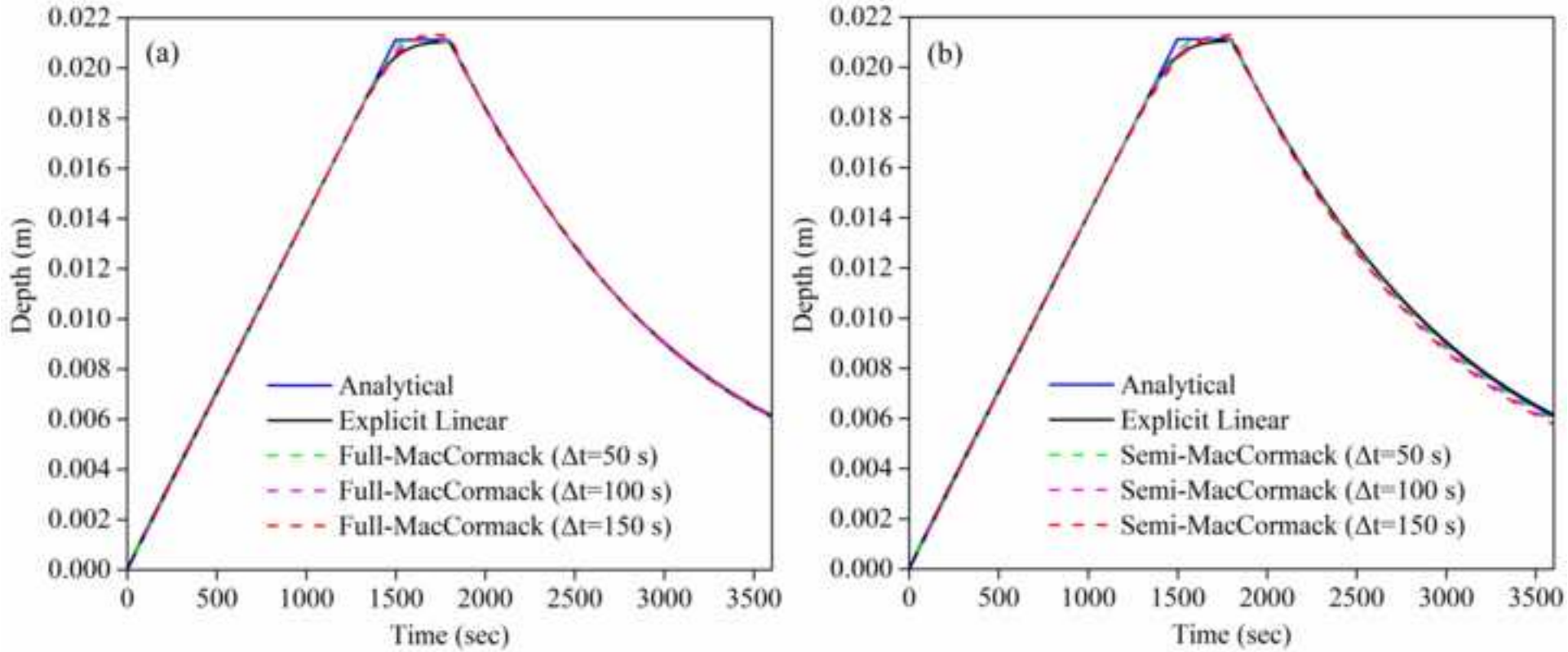

Figure 5
Click here to download high resolution image

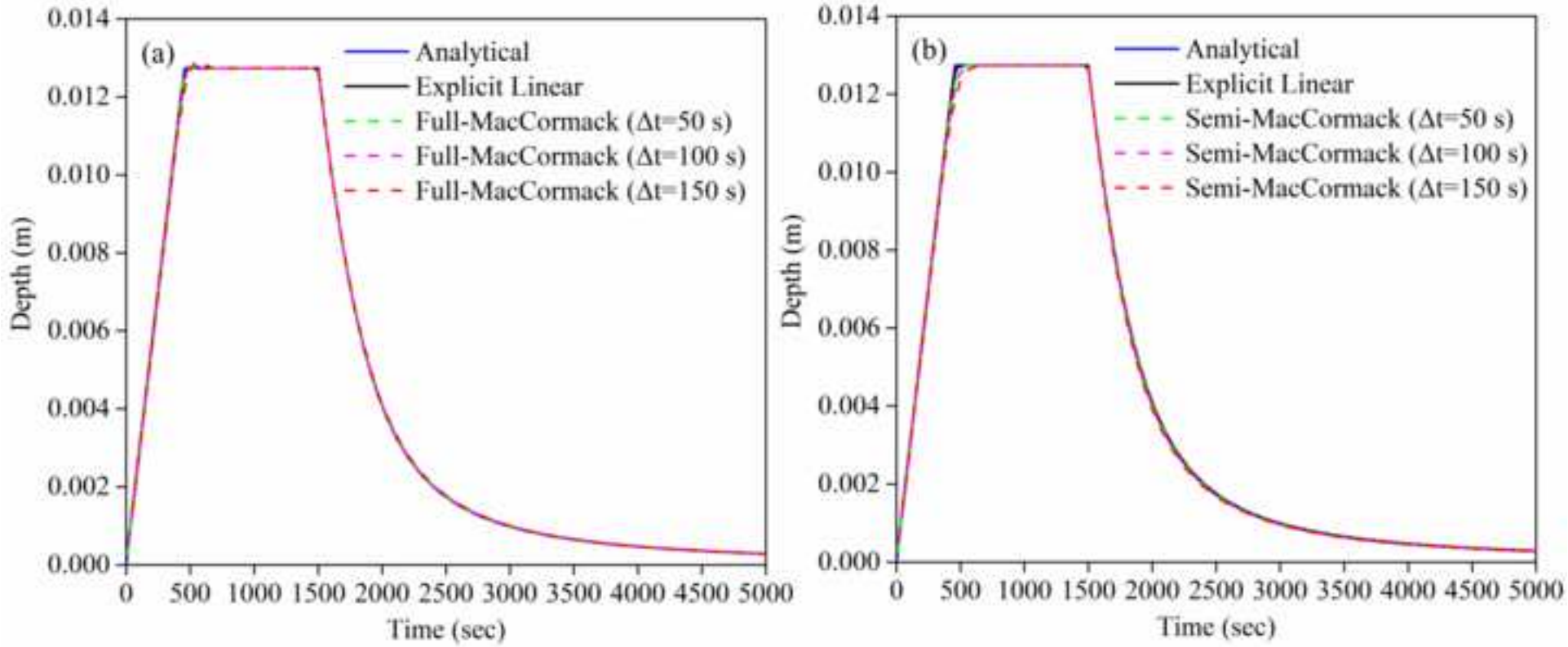

Figure 6

Click here to download high resolution image

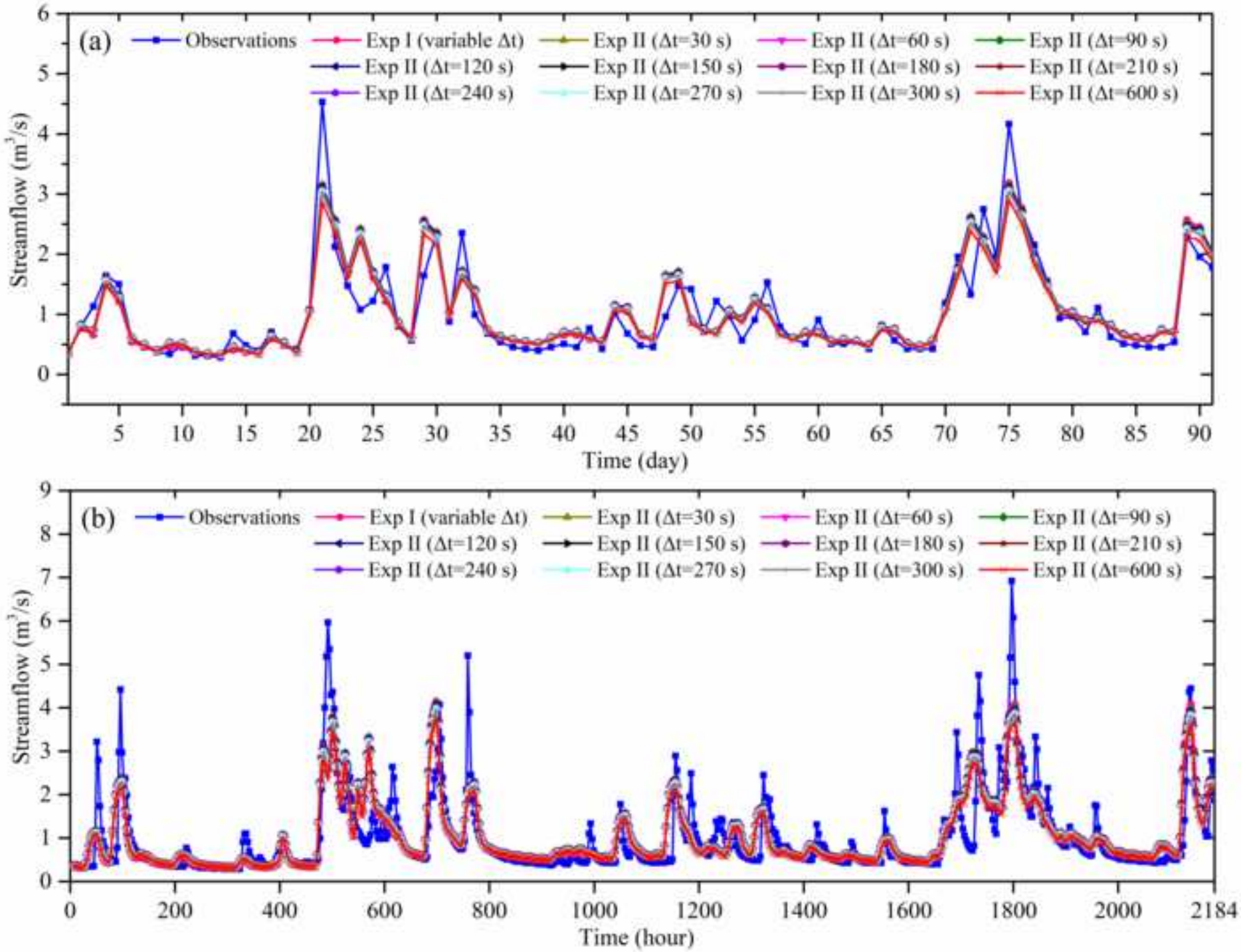

Figure 7
Click here to download high resolution image